

An AMSR-E Data Unmixing Method for Monitoring Flood and Waterlogging Disaster

GU Lingjia^{1,2}, ZHAO Kai¹, ZHANG Shuang², ZHENG Xingming¹

(1. Northeast Institute of Geography and Agroecology, Chinese Academy of Sciences, Changchun 130012, China;

2. College of Electronic Science & Engineering, Jilin University, Changchun 130012, China)

Abstract: Spectral remote sensing technique is usually used to monitor flood and waterlogging disaster. Although spectral remote sensing data have many advantages for ground information observation, such as real time and high spatial resolution, they are often interfered by clouds, haze and rain. As a result, it is very difficult to retrieve ground information from spectral remote sensing data under those conditions. Compared with spectral remote sensing technique, passive microwave remote sensing technique has obvious superiority in most weather conditions. However, the main drawback of passive microwave remote sensing is the extreme low spatial resolution. Considering the wide application of the Advanced Microwave Scanning Radiometer-Earth Observing System (AMSR-E) data, an AMSR-E data unmixing method was proposed in this paper based on Bellerby's algorithm. By utilizing the surface type classification results with high spatial resolution, the proposed unmixing method can obtain the component brightness temperature and corresponding spatial position distribution, which effectively improve the spatial resolution of passive microwave remote sensing data. Through researching the AMSR-E unmixed data of Yongji County, Jilin Province, Northeast China after the worst flood and waterlogging disaster occurred on July 28, 2010, the experimental results demonstrated that the AMSR-E unmixed data could effectively evaluate the flood and waterlogging disaster.

Keywords: passive microwave unmixing method; flood and waterlogging disaster; surface type classification; AMSR-E; MODIS; Yongji County of Jilin Province

Citation: Gu Lingjia, Zhao Kai, Zhang Shuang, Zheng Xingming, 2011. An AMSR-E data unmixing method for monitoring flood and waterlogging disaster. *Chinese Geographical Science*, 21(6): 666–675. doi: 10.1007/s11769-011-0463-3

1 Introduction

Among a variety of natural disasters, flood and waterlogging is one of main disaster that do serious harm to national economy and human being living. In order to monitor and evaluate flood disasters, it is very important to acquire and analyze the relative data information in time. However, the traditional methods based on manual acquisition are not suitable for flood disaster research due to the demands of the process of data acquisition and data precision. Remote sensing techniques play an active and important role in flood disaster management, such as monitoring, emergency response and evaluation,

mainly using the optical sensor or microwave radar. At present, spectral remote sensing and aerial remote sensing techniques are adopted mostly to enhance the integrated ability of monitoring, precaution and emergency response for flood disaster. The spectral remote sensing data with high spatial resolution, such as LANDSAT thematic mapper (LANDSAT-TM), SPOT high resolution visible (SPOT-HRV) and Quick Bird, or those with high time resolution, such as the moderate resolution imaging spectroradiometer (MODIS) and the advanced very high resolution radiometer (AVHRR) are often used in the researches on flood and waterlogging disaster (Tan *et al.*, 2004; Rahman *et al.*, 2007; Bindlish *et al.*,

Received date: 2010-09-30; accepted date: 2010-12-29

Foundation item: Under the auspices of National Natural Science Foundation of China (No. 40971189), Knowledge Innovation Programs of Chinese Academy of Sciences (No. KZCX2-YW-340), China Postdoctoral Science Foundation (No. 20100471276)

Corresponding author: ZHAO Kai. E-mail: zhaokai@neigae.ac.cn

© Science Press, Northeast Institute of Geography and Agroecology, CAS and Springer-Verlag Berlin Heidelberg 2011

2009; Nishat and Rahman, 2009). Although spectral remote sensing technique has many advantages for analyzing the water characteristics derived from flooded area (Sun, 2002; Dey *et al.*, 2008; Ferrazzoli *et al.*, 2010), such as real time and high spatial resolution, spectral remote sensing images are often interfered by clouds, haze and rain. As a result, it is difficult to retrieve ground information from spectral remote sensing data under those conditions. In contrast, passive microwave has the capacity to penetrate cloud cover, dust, and haze (Ulaby *et al.*, 1986). Passive microwave remote sensing is often used to observe microwave emission features from the surface of the Earth under most weather conditions. Surface types can be classified effectively by analyzing the scattering and emissivity of microwave signals from different surface characteristics. Furthermore, passive microwave remote sensing data are also used to retrieve other interrelated geophysical parameters, such as land surface temperature, soil moisture, and vegetation (Christopher *et al.*, 1990). Other advantages of passive microwave remote sensing include short data acquisition period and long-term geophysical record, both of which play an important role in monitoring climate change.

Although passive microwave remote sensing technique has obvious superiority in most weather conditions, it has low spatial resolution. Compared to the large number of spectral unmixing models, there are only a small number of unmixing models for microwave remote sensing data. These unmixing methods mainly use the deconvolve technique based on the antenna pattern of microwave remote sensor (Farrar and Smith, 1992). Moreover, these methods do not depend on the prior knowledge of surface types, but work at the expense of detection sensitivity. For example, Bellerby *et al.* (1998) obtained land and sea brightness temperature only from mixed pixels in Special Sensor Microwave/Imager (SSM/I) data, without consideration of surface type classification results.

In order to improve spatial resolution of microwave remote sensing data, based on Bellerby's algorithm, an Advanced Microwave Scanning Radiometer-Earth Observing System (AMSR-E) data unmixing method was proposed to monitor flood and waterlogging disaster in this paper. By utilizing the surface type classification results with high spatial resolution, and by combining a mathematical unmixing model of passive microwave

data, the component brightness temperature and corresponding spatial positions were computed. Through analyzing the AMSR-E unmixed data from the flood and waterlogging disaster of Yongji County, Jilin Province, Northeast China in 2010, the effectiveness of the AMSR-E data unmixing method was assessed.

2 Study Area and Data

2.1 Study area

Yongji County is located in Jilin Province, Northeast China (Fig. 1), lying in the transitional zone from the Songnen Plain to the Changbai Mountains. The county covers an area of approximately 2629 km². It has a typical warm continental monsoon climate. The mean annual temperature is 4.9°C and the mean annual precipitation is 696.6 mm. Water area and forest land area cover 4.9% and 48.3% of the total land area, respectively (Zhang *et al.*, 2006). Yongji County suffered from a rarely severe flood disaster on July 28, 2010. Kouqian town, the administrative center of the county, has experienced a largest flood occurring once every 1600 years, with 12-hour precipitation up to more than 290 mm.

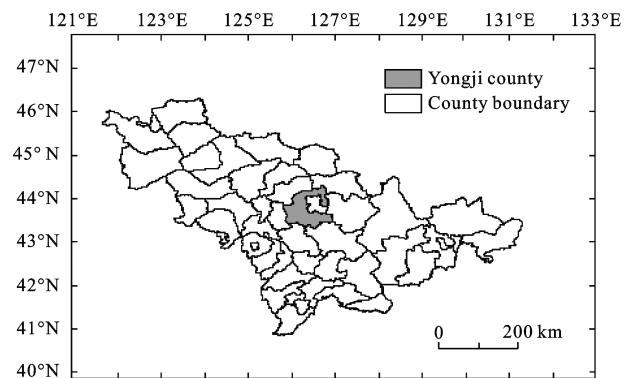


Fig. 1 Location of Yongji County in Jilin Province, China

2.2 Data

2.2.1 MODIS data

In this research, MOD09A1 products were selected from Land Process Distributed Active Archive Center (LPDAAC). MOD09A1 data provided an estimate of the surface spectral reflectance and its spatial resolution is 500 m. In the 8-day product, each surface reflectance pixel contained the best observation results with high observation coverage, low view angle, the absence of

clouds or cloud shadow and aerosol loading. According to the geographical location of Yongji County, the 8-day MOD09A1 products with acquisition dates from July 13 to July 20, from July 21 to July 28 and from July 29 to August 5, 2010 were selected, which were in accordance with the dates before, during and after the flood disaster. Moreover, the seven bands of MOD09A1 were processed using the MODIS reprojection tool (MRT). Resampling type was the nearest neighbor, projection type was geographic, and selected datum was WGS-84. After processing, the spatial resolution of each grid pixel was $0.0025^\circ \times 0.0025^\circ$. Similarly, two bands of MOD09Q1 data in the same periods were processed. The composite MODIS color images are shown in Fig. 2, they represent the images before, during and after the flood disaster.

As shown in Fig. 2b, Yongji County almost covered with heavy clouds during the flood in 2010. Because of cloud interference, the ground information could not be detected in the cloudy weather. Under this condition, spectral remote sensing technique was not suitable for monitoring ground information. From Fig. 2c, it can be seen that the ground information of Yongji County was clearly seen because there were less cloud interference after the disaster. The green regions denote vegetation coverage areas, while the yellow regions represent flooded areas.

2.2.2 AMSR-E data

AMSR-E is a twelve-channel, six-frequency, passive-microwave radiometer system. This system measures polarized brightness temperature horizontally and vertically at 6.9 GHz, 10.7 GHz, 18.7 GHz, 23.8 GHz, 36.5 GHz and 89.0 GHz. Spatial resolutions of the individual measurements varied from 5.4 km at 89.0 GHz to 56.0

km at 6.9 GHz (Kawanishi *et al.*, 2003). The brightness temperature data derived from AMSR-E L2A product were first selected. The data acquisition dates of AMSR-E were every two days from July 20 to August 9, 2010 with descending orbit global data. The spatial resolution of AMSR-E data was 25 km and was interpolated into regular grids of $0.25^\circ \times 0.25^\circ$ using EASE-GRID projection. Considering the sensitivity of low-frequency microwave emission to surface information, the 10.7 GHz horizontal polarization data of AMSR-E were selected as test data. From Fig. 3, it can be seen that the AMSR-E pixel amount of Yongji County is less than 20 because of its low spatial resolution.

The corresponding AMSR-E data of Yongji County in every two days are shown in Fig. 4. It can be seen that the AMSR-E brightness temperature data on July 28, 2010 were the lowest, which was in accordance with the date of practical rainstorm in Yongji County. Passive microwave remote sensing data may be able to effectively monitor ground information changes as compared to data from spectral remote sensing in cloudy or rainy weather, thus, AMSR-E data can be used to realize real-time monitoring for the study area, and the brightness temperature data derived from a long period of observation can be used to establish the brightness temperature database. Through the comparison between practical data and history data, unusual ground situation can be warned in advance.

3 AMSR-E Data Unmixing Method

3.1 Background

The AMSR-E sensor provides measurements of terrestrial, oceanic, and atmospheric parameters for the inves-

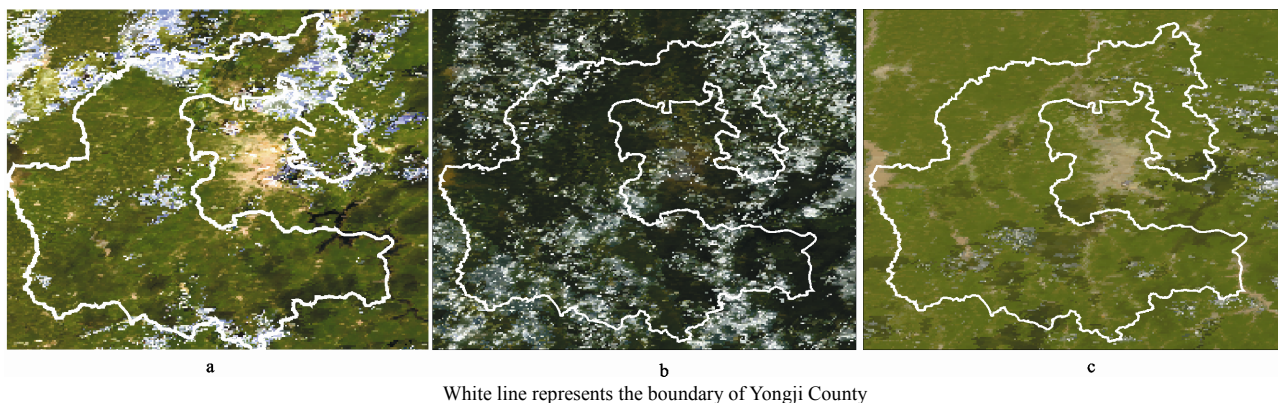


Fig. 2 MODIS color images of Yongji County before (a), during (b) and after (c) flood disaster

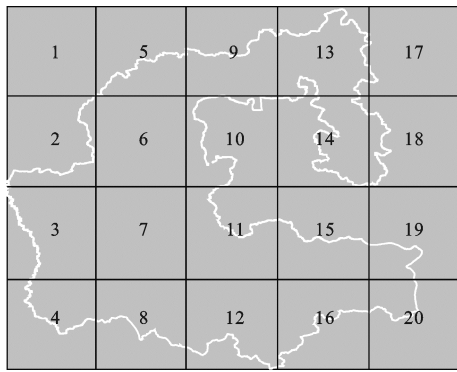


Fig. 3 Distribution of observation points in Yongji County

tigation of global water and energy cycles, including precipitation rate, sea surface temperature, sea ice concentration, snow water equivalent, soil moisture, surface wetness, wind speed, atmospheric cloud water, water vapor, *etc.* AMSR-E data have been widely applied in microwave remote sensing field. The spatial resolution of AMSR-E data is approximately 25 km. As a result, the brightness temperature value of each AMSR-E pixel represents the mixed brightness temperature of a large region. In order to obtain high-precision retrieval result, the brightness temperature of each component should be computed (Xu *et al.*, 2000; Song and Zhao, 2004). Bellerby *et al.* (1998) obtained land and sea brightness temperatures from mixed coastal pixels in SSM/I data. The designed model assumes that land and sea have an independent, but similarly uniform component brightness temperature in neighbor nine pixels. Although the

Bellerby's algorithm controlled the selection of nine mixed pixels, the main error was caused by assuming that land and sea brightness temperature were uniform over a nine-pixel area. Furthermore, the method only separated land and sea component brightness temperature from the mixed coastal region and did not realize the separation of water and land in inland region. Based on the theory of Bellerby, a new passive microwave unmixing model utilizing surface type classification with high spatial resolution is proposed in this study.

3.2 Surface type classification

Surface type classification results should be obtained in advance for the proposed unmixing method. Because the geophysical parameter of land is relatively stable, land surface type can be accurately classified at a certain spatial scale and in a certain time period. As a result, the surface type of observation area can be classified well by using the land resources utilization results combined with the surveyed results in a certain time period. For the study area were abundant in water and vegetation resources, the surface types were classified into water and vegetation types in this study. MODIS products with middle spatial resolution were used to obtain the surface classification results. Here, normalized difference vegetation index (NDVI) and combined index of NDVI and near-infrared for water body identification (CIWI) were used to identify water and vegetation.

(1) NDVI: Vegetation index has high absorption in

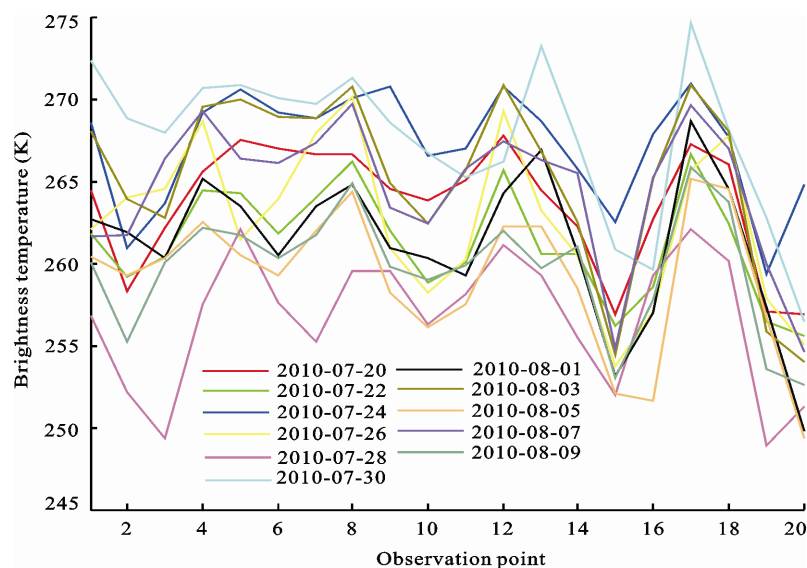


Fig. 4 AMSR-E brightness temperature data in Yongji County

visible red light (Red) and strong reflectance in near-infrared light (NIR). NDVI is described as Equation (1) (Alecu *et al.*, 2005; Ding *et al.*, 2007):

$$NDVI = (NIR - Red) / (NIR + Red) \\ = (B_2 - B_1) / (B_2 + B_1) \quad (1)$$

where B_1 is the first band of MODIS representing the visible red band; B_2 is the second band of MODIS representing the near-infrared band. If NDVI is less than zero, surface type is defined as water type; if NDVI is greater than zero, surface type is defined as vegetation type.

(2) CIWI: According to the band characteristics of MODIS data, researchers proposed CIWI through analyzing the spectrum and image of water body (Mo *et al.*, 2007; Liao and Liu, 2008; Song *et al.*, 2008). CIWI is described as Equation (2):

$$CIWI = NDVI + B_7 / \bar{B}_7 + C \quad (2)$$

where B_7 represents the seventh band information of MODIS data; \bar{B}_7 denotes the average value of the seventh band information; C is a constant value. If CIWI is less than zero, surface type is defined as water type, otherwise defined as vegetation type.

Because the MODIS 8-day composite image from July 21 to July 28 was almost covered by clouds, the MODIS 8-day images before July 21 and that after July 28 were processed respectively to obtain the surface type classification results before and after the flood disaster. Water remote sensing images can be obtained by using the classification results combined with original bands (Fig. 5). In Fig. 5c, white pixels represent original water areas and blue pixels represent the additional water areas caused by the flood disaster. In general, water areas change less with the spatial variation and most

with time variation. In the flood disaster period, water areas changed to a great extent and satisfied a special rule. The most increased water areas resulted from the expansion of the original water areas, and the remaining increased water areas were related to the low topography of flooded region.

Because AMSR-E data can effectively monitor ground information under most weather conditions, by combining AMSR-E data with the original water areas of Fig. 5c, the observation points 2, 3, 7, 15, 19 and 20 of Fig. 3 were selected. As shown in Fig. 6, the AMSR-E data of the selected points can dynamically reflect the water changes during the observation period. Usually, the decreased brightness temperature value of AMSR-E data reflects the increased proportion of water. On the contrary, the increased brightness temperature value of AMSR-E data reflects the decreased proportion of water. Therefore, AMSR-E data can be used to estimate the change trend of surface type in a certain time period based on the existing surface classification results.

3.3 Unmixing model

Firstly, the surface classification data with high spatial resolution were matched with AMSR-E brightness temperature with low spatial resolution by utilizing the geographical position information (Minghelli-Roman *et al.*, 2006; Swarvanu and Qu, 2006; Zurita-Milla *et al.*, 2008; Gu *et al.*, 2011). Given the pixel numbers of the two components (vegetation and water) in AMSR-E mixed pixel, the proportion of the two surface types were computed by equations (3) and (4):

$$P_{\text{green}} = \frac{N_{\text{green}}}{(R_{\text{low}} / R_{\text{high}})^2} \quad (3)$$

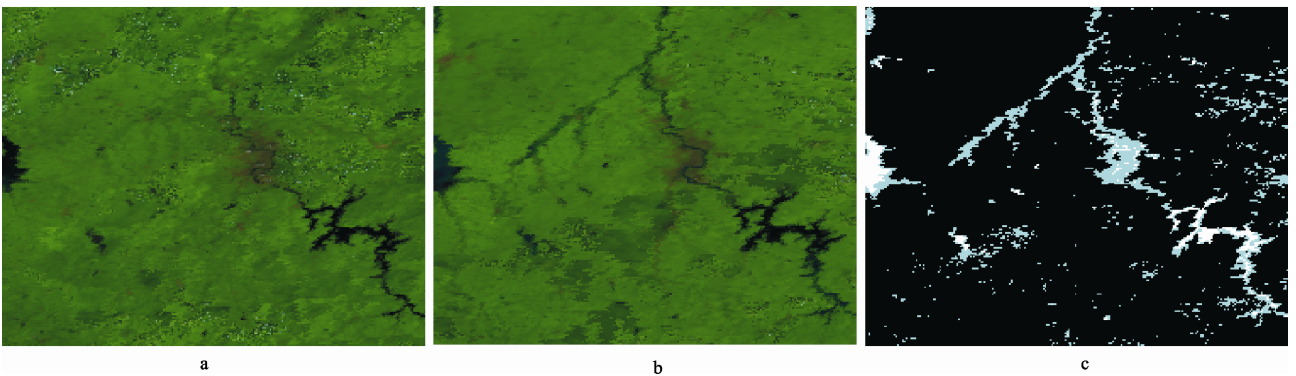


Fig. 5 Water remote sensing images before (a) and after (b) flood disaster and water change trend image (c) in Yongji County

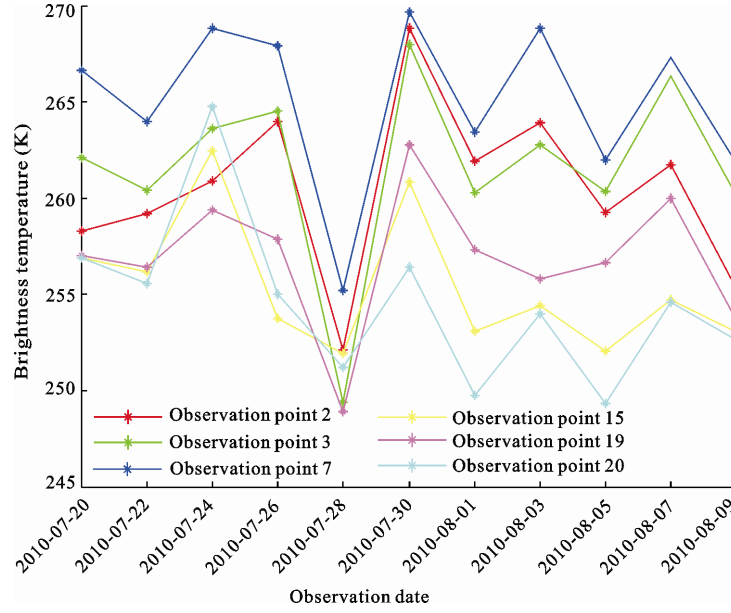


Fig. 6 AMSR-E data of the water observation points

$$P_{\text{water}} = 1 - P_{\text{green}} \quad (4)$$

where P_{green} represents the vegetation component proportion of AMSR-E mixed pixel; N_{green} denotes the number of vegetation component; R_{high} is the high spatial resolution of the surface classification data; R_{low} represents the low spatial resolution of AMSR-E mixed pixel; and P_{water} is the water component proportion of the AMSR-E mixed pixel. Finally, the proportions and high spatial resolution positions of the two components were obtained.

Furthermore, the $m \times n$ AMSR-E mixed pixels were selected as a sliding window and the proportions of the different surface types corresponding to each AMSR-E mixed pixel as component proportion matrices were recorded (Xu *et al.*, 2001; Maaß and Kaleschke, 2010). These matrices contain the proportions of each of the two components that fall within one mixed AMSR-E pixel inside the $m \times n$ window. In general, water brightness temperature maintains relative stabilization in the nearest regions. As a result, brightness temperature values of water component were assumed to be uniform in the sliding window. Furthermore, the passive microwave unmixing model was built as Equation (5):

$$TB(i, j) = P_{\text{green}}(i, j)T_{\text{green}}(i, j) + P_{\text{water}}(i, j)T_{\text{water}} \quad (i = 1, 2, \dots, m; j = 1, 2, \dots, n) \quad (5)$$

where $TB(i, j)$ is AMSR-E mixed brightness temperature of $m \times n$ sliding window, known vectors; $P_{\text{green}}(i, j)$ is

vegetation component proportion of each mixed AMSR-E pixel located in $m \times n$ sliding window, known vector; $T_{\text{green}}(i, j)$ is vegetation brightness temperature of each mixed AMSR-E pixel located in $m \times n$ sliding window, unknown vector; $P_{\text{water}}(i, j)$ is water component proportion of each mixed AMSR-E pixel located in $m \times n$ sliding window, known vector; and T_{water} is water brightness temperature of each mixed AMSR-E pixel located in $m \times n$ sliding window, unknown vector.

If $P_{\text{water}} = 1$ or $P_{\text{green}} = 1$ for all AMSR-E mixed pixels located in the $m \times n$ sliding window, then the AMSR-E pixels were regarded as pure pixels and were not unmixed.

As shown in the proposed passive microwave unmixing model, there are $m \times n + 1$ unknown vectors ($T_{\text{green}}(i, j)$, T_{water}) for $m \times n$ equations. This is a linear system of equations that has fewer equations than variables, known as an underdetermined system of equations. The system may have infinite solutions, thus determining the optimal solution is the key problem in the proposed model.

Here, a method that can search for the optimal solution in entire solutions was presented. In order to determine the initial brightness temperature range, k-mean clustering was used to classify all AMSR-E mixed pixels. The two centroids of the k-mean clustering results denote the brightness temperature statistics of the two components, recorded as C_{green} and C_{water} . At the same

time, the average, maximum, minimum, standard deviation, and component proportions in the $m \times n$ sliding window were computed. Furthermore, the change threshold of vegetation brightness temperature (L_{green}) was obtained based on each component proportion. Moreover, the initial selection range of T_{green} was determined as $[C_{\text{green}} - L_{\text{green}}, C_{\text{green}} + L_{\text{green}}]$. Similarly, the change threshold of water brightness temperature L_{water} and its initial selection range $[C_{\text{water}} - L_{\text{water}}, C_{\text{water}} + L_{\text{water}}]$ were obtained. Moreover, water brightness temperature should be lower than vegetation brightness temperature, therefore, it should satisfy $(C_{\text{water}} + L_{\text{water}}) < (C_{\text{green}} - L_{\text{green}})$.

In addition, an accuracy measure was also designed to evaluate optimal solution as follows:

$$R = \sqrt{\sum_{i=1}^m \sum_{j=1}^n (TB(i, j) - P_{\text{green}}(i, j)T_{\text{green}}(i, j) - P_{\text{water}}(i, j)T_{\text{water}})^2} < \xi \quad (6)$$

where R is the objective function; and ξ is the given error and its value determines the solution precision.

The optimal solution should also satisfy the following equation:

$$T_{\text{water}} < T_{\text{green}}(i, j) \quad (i = 1, 2, \dots, m; j = 1, 2, \dots, n) \quad (7)$$

The initial component values were chosen and used to substitute Equation (5) under the union constraint of equations (6) and (7). The optimal solution was obtained by using the least square method and iterative computation. The relationship between mixed pixel and the two components was taken into account when determining initial brightness temperature ranges. Moreover, there were several conditions that constrain the solution range

of the equations. Thus, the proposed unmixing model may be able to obtain a better solution through the iterative process and by solving the underdetermined system of equations.

4 Experimental Results

The surface type classification data after the flood disaster with different spatial resolution, i.e. 5 km, 1 km, 500 m and 250 m, were used to unmix AMSR-E data of Yongji County. The results of mixed and unmixed images and data histograms with the acquisition date of July 30, 2010 are shown in Fig. 7 and Fig. 8. From Fig. 7 and Fig. 8, it can be seen that the spatial resolution of the AMSR-E data of Yongji County get prominently improve by the proposed unmixing method. The lower brightness temperature of AMSR-E unmixed data represents the greater water proportion.

By comparison Fig. 8g and Fig. 2c, the flood disaster area distribution of the spectral image and that of the microwave unmixed image are basically consistent. The disaster area of flood and waterlogging based on AMSR-E unmixed data was approximately 56 400 ha. According to the official publication information, the disaster area was 56 000 ha in Yongji County on July 30, 2010. The experimental results demonstrate that the AMSR-E unmixed data can effectively evaluate the flood disaster.

5 Discussion and Conclusions

Compared with Bellerby's algorithm, the proposed unmixing method can obtain the component brightness

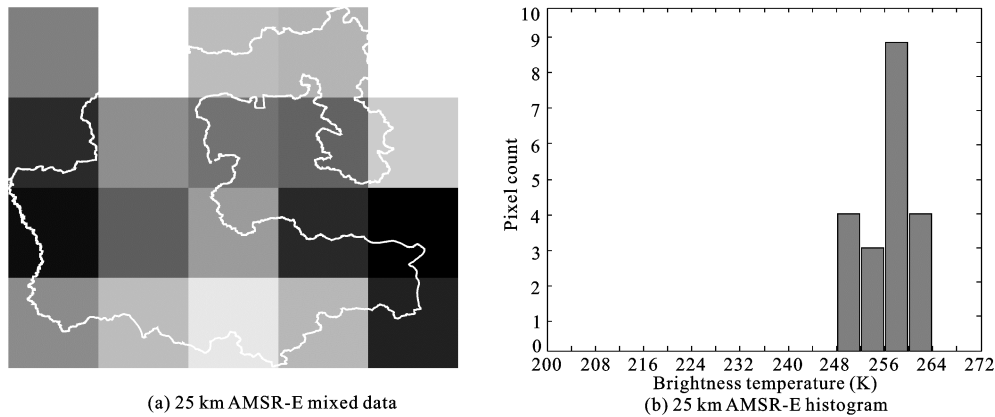


Fig. 7 AMSR-E mixed data

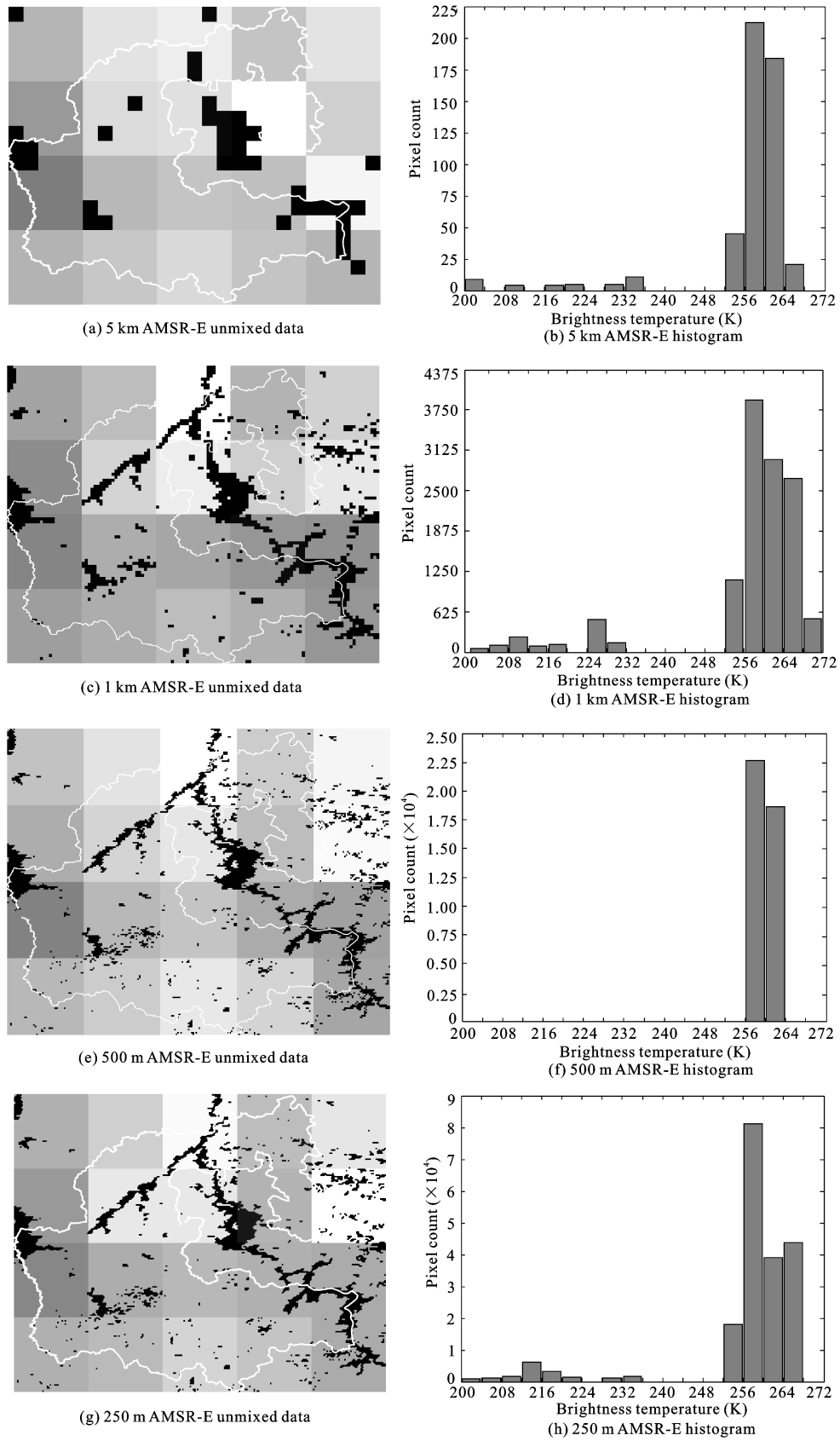


Fig. 8 AMSR-E unmixed data based on classification data with different spatial resolution

temperature and corresponding spatial position distribution. Furthermore, Bellerby assumed that the brightness temperature values of the two components were full uniform in neighbor nine pixels, while the proposed method only assumed that water brightness temperature value was uniform in neighbor pixel. Therefore, the data precision using the proposed method is better than that using Bellerby's algorithm. The proposed method can separate water and vegetation brightness temperature from inland area, and can separate land and sea brightness temperature from mixed coastal pixels. However, the surface classification results with high spatial resolution should be obtained before using the proposed method.

In this paper, the surface classification results were obtained based on MODIS image data. Because the topography and physiognomy of the observation area are relatively stable in a certain time and spatial scales, through researching the long-term statistic results of the observation area, the change trend of surface type could be predicted based on AMSR-E data with 25 km spatial resolution. Furthermore, the dynamic change model between the microwave data and surface classification results should be established. If the predicted results of surface type classification are applied to the passive microwave unmixing model, the influence of surface type classification result on unmixing accuracy will be reduced. These researches would be done in the future.

The proposed unmixing method can effectively improve the spatial resolution of passive microwave remote sensing data, meanwhile, remain monitoring advantages of microwave technique. The microwave unmixed data with high spatial resolution can monitor the observation area well in a long period, which solves the monitoring effectiveness problems of spectral remote sensing data caused by clouds interferences. The monitoring method using the integrated advantages of spectral and microwave remote sensing have wide application prospects and potentials in monitoring flood and waterlogging disaster.

References

- Alecu Corina, Oancea Simona, Bryant Emily, 2005. Multi-resolution analysis of MODIS and ASTER satellite data for water classification. *Proceedings of SPIE—The International Society for Optical Engineering*, 5983: 59831Z. doi: 10.1117/12.649848
- Bellerby T, Taberner M, Wilmshurst A et al., 1998. Retrieval of land and sea brightness temperatures from mixed coastal pixels in passive microwave data. *IEEE Transactions on Geoscience and Remote Sensing*, 36(6): 1844–1851. doi: 10.1109/36.729355
- Bindlish R, Crow W T, Jackson T J, 2009. Role of passive microwave remote sensing in improving flood forecasts. *IEEE Geoscience and Remote Sensing Letters*, 6(1): 112–116. doi: 10.1109/LGRS.2008.2002754
- Christopher M U Neale, Marshall J Mcfarland, Chang Kai, 1990. Land-surface-type classification using microwave brightness temperatures from the special sensor microwave/imager. *IEEE Transaction on Geoscience and Remote Sensing*, 28(5): 829–838. doi: 10.1109/36.58970
- Dey Chandrama, Jia Xiuping, Fraser Donald, 2008. Decision fusion for reliable flood mapping using remote sensing images. *Proceeding—Digital Image Computing: Techniques and Applications*, DICTA 2008, 184–190. doi: 10.1109/DICTA.2008.65
- Ding Lidong, Yu Wenhua, Qin Zhihao et al., 2007. The mapping of flood remote sensing image based on MODIS in Poyang lake region. *Remote Sensing for Land & Resources*, 18(1): 82–85. (in Chinese)
- Farrar M R, Smith E A, 1992. Spatial resolution enhancement of terrestrial features using deconvolved SSM/I microwave brightness temperatures. *IEEE Transactions on Geoscience and Remote Sensing*, 30(2): 349–355. doi: 10.1109/36.134084
- Ferrazzoli P, Rahmoune R, Grings F et al., 2010. AMSR-E observations of rain and flood events over vegetated areas of LA Plata basin. *Microwave Radiometry and Remote Sensing of the Environment*, (special issue): 63–66. doi: 10.1109/MICRORAD.2010.5559588
- Gu lingjia, Zhao Kai, Zhang Shuwen et al., 2011. Comparative analysis of microwave brightness temperature data in Northeast China using AMSR-E and MWRI products. *Chinese Geographical Science*, 2011, 21(1): 84–93. doi: 10.1007/s11769-011-0442-8
- Kawanishi T, Sezai T, Ito Y et al., 2003. The advanced microwave scanning radiometer for the Earth Observing System (AMSR-E), NASDA's contribution to the EOS for global energy and water cycle studies. *IEEE Transactions on Geoscience and Remote Sensing*, 41(2): 184–194. doi: 10.1109/TGRS.2002.808331
- Liao Chenghao, Liu Xuehua, 2008. An effectiveness comparison between water body indices based on MODIS data. *Remote Sensing for Land & Resources*, 19(4): 22–26. (in Chinese)
- Maaß Nina, Kaleschke Lars, 2010. Improving passive microwave sea ice concentration algorithms for coastal areas: Applications to the Baltic Sea. *Tellus Series A Dynamic Meteorology and Oceanography*, 62(4): 393–410. doi: 10.1111/j.1600-0870.2010.00452.x
- Minghelli-Roman A, Polidori L, Mathieu-Blanc S et al., 2006. Spatial resolution improvement by merging MERIS-ETM images for coastal water monitoring. *IEEE Geoscience and Remote Sensing Letters*, 3(2): 227–231. doi: 10.1109/LGRS.

- 2005.861699
- Mo Weihua, Sun Han, Zhong Shiquan *et al.*, 2007. Research on the CIWI model and its application. *Remote Sensing Information*, (5): 16–21. (in Chinese)
- Nishat Bushra, Rahman S M Mahbubur, 2009. Water resources modeling of the Ganges-Brahmaputra-Meghna river basins using satellite remote sensing data. *Journal of the American Water Resources Association*, 45(6): 1313–1327. doi: 10.1111/j.1752-1688.2009.00374.x.
- Rahman S, Rahman H, Keramat M, 2007. Study on the seasonal changes of land cover and their impact on surface albedo in the northwestern part of Bangladesh using remote sensing. *International Journal of Remote Sensing*, 28(5): 1001–1022. doi: 10.1080/01431160600810880.
- Song Xiaoning, Huang Shifeng, Liu Qinhuo *et al.*, 2008. Vegetation water inversion using MODIS satellite data. *2007 IEEE International Geoscience and Remote Sensing Symposium, IGARSS 2007*, 1865–1868. doi: 10.1109/IGARSS.2007.4423187
- Song Xiaoning, Zhao Yingshi, 2004. Inversion of component temperatures based on MODIS data. *Journal of China University of Mining & Technology*, 33(4): 406–411. (in Chinese)
- Sun Shaocheng, 2002. Applications of remote sensing in flooding alleviation system in China. *Progress in Geography*, 21(3): 282–288. (in Chinese)
- Swarvanu Dasgupta, Qu John J, 2006. Combining MODIS and AMSR-E based vegetation moisture retrievals for improved fire risk monitoring. *SPIE-The International Society for Optical Engineering*, 6298: 814–816. doi: 10.1117/12.681147
- Tan Qulin, Bi Siwen, Hu Jiping *et al.*, 2004. Measuring lake water level using multi-source remote sensing images combined with hydrological statistical data. *International Geoscience and Remote Sensing Symposium (IGARSS)*, 7: 4885–4888. doi: 10.1109/IGARSS.2004.1370258
- Ulaby F T, Moore R K, Fung A K, 1986. *Microwave Remote Sensing: Active and Passive, Volume II: Radar Remote Sensing and Surface Scattering and Emission Theory*. MA: Artech House Publishers, 200–210.
- Xu Xiru, Chen Liangfu, Zhuang Jiali, 2001. Genetic inverse algorithm for retrieval of component temperature of mixed pixel by multi-angle thermal infrared remote sensing data. *Science in China (Series D)*, 44(4): 364–372. doi: 10.1007/BF02907107
- Xu Xiru, Zhuang Jiali, Chen Liangfu, 2000. The multi-angle thermal infrared remote sensing and retrieval of component temperatures of mixed Pixel. *Acta Scientiarum Naturalium Universitatis Pekinensis*, 36(4): 556–560. (in Chinese)
- Zhang Shuwen, Zhang Yangzhen, Li Ying *et al.*, 2006. *Land Use/Cover Spatial Character Analyzing Based on Northeast China*. Beijing: Science Press, 25–37. (in Chinese)
- Zurita-Milla R, Clevers J, Schaepman M E *et al.*, 2008. Unmixing-based landsat TM and MERIS FR data fusion. *IEEE Transactions on Geoscience and Remote Sensing*, 5(3): 453–457. doi: 10.1109/LGRS.2008.919685